REPORT DOCUMENTATION PAGE

Form Approved
OMB No. 0704-0188

1. REPORT DATE *(DD-MM-YYYY)*	2. REPORT TYPE	3. DATES COVERED *(From - To)*
19-08-2011	Book Chapter	

4. TITLE AND SUBTITLE

The Design of Non-Wetting Surfaces with FluoroPOSS

5a. CONTRACT NUMBER

5b. GRANT NUMBER

5c. PROGRAM ELEMENT NUMBER

6. AUTHOR(S)
Anush Tuteja (Univ. of Michigan, Ann Arbor) and Joseph M. Mabry

5d. PROJECT NUMBER

5f. WORK UNIT NUMBER
23030521

7. PERFORMING ORGANIZATION NAME(S) AND ADDRESS(ES)

Air Force Research Laboratory (AFMC)
AFRL/RZSM
9 Antares Road
Edwards AFB CA 93524-7401

8. PERFORMING ORGANIZATION REPORT NUMBER

AFRL-RZ-ED-BK-2011-366

9. SPONSORING / MONITORING AGENCY NAME(S) AND ADDRESS(ES)

Air Force Research Laboratory (AFMC)
AFRL/RZS
5 Pollux Drive
Edwards AFB CA 93524-7048

10. SPONSOR/MONITOR'S ACRONYM(S)

11. SPONSOR/MONITOR'S NUMBER(S)
AFRL-RZ-ED-BK-2011-366

12. DISTRIBUTION / AVAILABILITY STATEMENT

Approved for public release; distribution unlimited (PA #11664).

13. SUPPLEMENTARY NOTES
Invited book chapter submission.

14. ABSTRACT

Functional non-wetting materials are of interest for a diverse array of applications. It has long been understood that factors contributing to the wettability of a surface include surface free energy and surface roughness. More recently, surface texture has been found to be of equal or greater importance, especially if the desire is for the surface to repel low surface tension liquids, such as short-chain hydrocarbons and alcohols. This chapter will describe recent work in the design and production of wetting-resistant surfaces utilizing fluorinated Polyhedral Oligomeric SilSesquioxanes (FluoroPOSS), as well as the development of dimensionless design parameters to aid in the preparation of such surfaces. FluoroPOSS compounds are organic/inorganic hybrid materials that exhibit low surface energy attributes, as well as an octahedral structure, which results in useful migration and aggregation characteristics when blended into polymer matrices. Wetting-resistant surfaces containing FluoroPOSS are produced either by techniques that specifically incorporate all three critical parameters for wetting-resistance, or by the modification of substrates already possessing the desired surface texture.

15. SUBJECT TERMS

16. SECURITY CLASSIFICATION OF:			17. LIMITATION OF ABSTRACT	18. NUMBER OF PAGES	19a. NAME OF RESPONSIBLE PERSON
					Dr. Joseph M. Mabry
a. REPORT	b. ABSTRACT	c. THIS PAGE	SAR	22	19b. TELEPHONE NUMBER *(include area code)*
Unclassified	**Unclassified**	**Unclassified**			N/A

The Design of Non-Wetting Surfaces with FluoroPOSS

Anish Tuteja,[1]* Joseph M. Mabry[2]*

[1]Department of Materials Science and Engineering, University of Michigan, Ann Arbor, MI 48109

[2]Air Force Research Laboratory, Space and Missile Propulsion Division, Edwards AFB, CA 93524

Abstract Functional non-wetting materials are of interest for a diverse array of applications. It has long been understood that factors contributing to the wettability of a surface include surface free energy and surface roughness. More recently, surface texture has been found to be of equal or greater importance, especially if the desire is for the surface to repel low surface tension liquids, such as short-chain hydrocarbons and alcohols. This chapter will describe recent work in the design and production of wetting-resistant surfaces utilizing fluorinated Polyhedral Oligomeric SilSesquioxanes (FluoroPOSS), as well as the development of dimensionless design parameters to aid in the preparation of such surfaces. FluoroPOSS compounds are organic/inorganic hybrid materials that exhibit low surface energy attributes, as well as an octahedral structure, which results in useful migration and aggregation characteristics when blended into polymer matrices. Wetting-resistant surfaces containing FluoroPOSS are produced either by techniques that specifically incorporate all three critical parameters for wetting-resistance, or by the modification of substrates already possessing the desired surface texture.

X.1 Introduction

X.1.1 Non-wetting Surfaces

Non-wetting surfaces and materials that affect wetting-resistance are desirable for a wide variety of military, commercial, and specialty applications. The simplest measure of wetting on a smooth surface is the equilibrium contact angle θ, given by the Young's equation [1] as:

$$\cos\theta = \frac{\gamma_{sv} - \gamma_{sl}}{\gamma_{lv}} \qquad (1)$$

where γ refers to the interfacial tension and s, l and v refer to the solid, liquid and vapor phase, respectively. The solid-vapor interfacial tension (γ_{sv}) and the liquid-vapor interfacial tension (γ_{lv}) are also commonly referred to as the solid surface energy and the liquid surface tension, respectively. Smooth surfaces that display contact angles $\theta > 90°$ with water are considered hydrophobic, while smooth surfaces that display contact angles $\theta < 90°$ with water are considered hydrophilic. In recent years, a new class of '*superhydrophobic*' surfaces has emerged. These surfaces display contact angles greater than 150° and low contact angle hysteresis - the difference between the advancing and the receding contact angles [2,3]. Note that all superhydrophobic surfaces are textured (or rough), as the maximum water contact angle measured on a smooth surface is ~ 125°–130° [4-6]. Superhydrophobicity is pervasive in nature (see Figure 1) with various plant leaves [7-9], legs of the water strider [10-12], gecko's feet [13,14], troughs on the elytra of desert beetles [15] and insect wings [16] displaying this water-repelling characteristic.

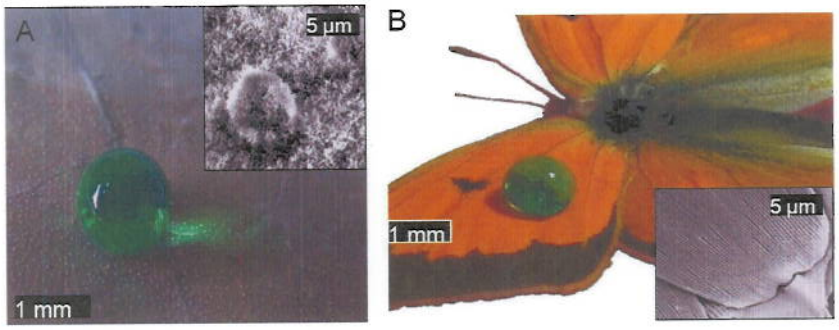

Fig.1 A. A droplet of water (colored green) on a superhydrophobic lotus leaf surface. The inset is an SEM image, highlighting the multiple scales of texture present on the lotus leaf surface. **B.** A droplet of water (colored green) on top of a butterfly (*Colias fieldi*) wing. The inset is an SEM image illustrating the texture of the butterfly wing. Images adapted from previous work.[17]

In a similar manner, based on their respective contact angles with oil, it is possible to classify surfaces as oleophilic ($\theta < 90°$), oleophobic ($\theta > 90°$) or superoleophobic ($\theta^* > 150°$). Here θ^* refers to the apparent contact angles i.e. the contact angle on a textured or rough surface. In spite of numerous natural superhydrophobic surfaces, there are no known naturally occurring oleophobic or superoleophobic surfaces. This is because oils possess significantly lower surface tension values than water and consequently spread on most natural and synthetic surfaces.

X.1.2 FluoroPOSS

Due to their low surface energy, fluorinated compounds are a logical choice when evaluating materials for use in the creation of non-wetting surfaces. Polyhedral molecules may also contribute positively to wetting resistance by helping to increase roughness in the produced surfaces. For these reasons, fluorinated polyhedra are highly desired. Polyhedral oligomeric silsesquioxane (POSS) [18] compounds are comprised of a silicon-oxygen core that is surrounded by organic functionality. They have received much interest as robust nanometer-sized building blocks for the development of high performance materials.[19-21] POSS compounds have been developed for use in several commercial, military, and specialty applications. [19-21]

For the purposes of this chapter, FluoroPOSS (Fluorinated Polyhedral Oligomeric SilSesquioxanes), are described as POSS cages that are surrounded by fluoroalkyl functional groups with no surrounding hydrocarbon periphery, other than the methylene groups immediately adjacent to the silicon atoms. There are several possible methods to produce a range of different fluorinated POSS (FluoroPOSS) compounds [22-25]. In one case, hepta(3,3,3-trifluoropropyl)tricycloheptasiloxane trisodium silanolate was used as an intermediate for the preparation of FluoroPOSS compounds by "corner-capping" with fluoroalkyltrichlorosilanes (Figure X.2). [22]

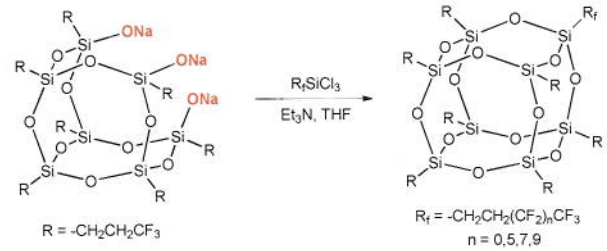

Fig. X.2 Synthesis of Fluorinated Polyhedral Oligomeric SilSesquioxanes (FluoroPOSS) compounds *via* "corner-capping" reaction of incompletely condensed POSS cages. Hepta(3,3,3-trifluoropropyl)tricycloheptasiloxane trisodium silanolate was isolated as an intermediate and reacted with fluoroalkyltrichlorosilanes of varying chain length. Reaction with (3,3,3-trifluoropropyl)trichlorosilane, in the presence of triethylamine, produces octahedral (3,3,3-trifluoropropyl)$_8Si_8O_{12}$ (Fluoropropyl POSS). Reaction with trichlorosilanes of longer fluoroalkyl chain length results in unsymmetrical, completely-condensed FluoroPOSS compounds. Branched and ether containing fluoroalkyl groups have also been attached using this method.

Another synthetic method produces octameric FluoroPOSS cages directly from the starting silanes *via* the single-step, base-catalyzed condensation reaction of

trialkoxysilanes to produce nearly quantitative yields of (1H,1H,2H,2H-heptadecafluorodecyl)$_8$Si$_8$O$_{12}$ POSS (Fluorodecyl POSS or Fluorodecyl$_8$T$_8$). [24]

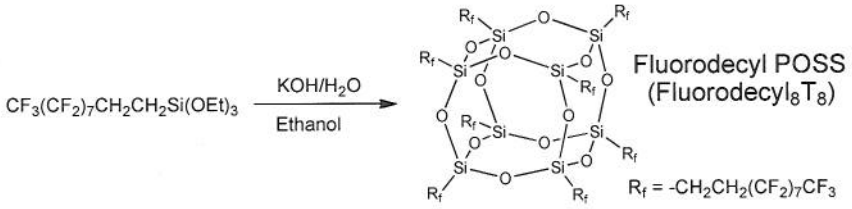

Fig. X.3 Direct synthesis of octameric Fluorodecyl POSS *via* the base-catalyzed condensation reaction of (1H,1H,2H,2H-heptadecafluorodecyl)triethoxysilane in alcoholic solvent to produce (1H,1H,2H,2H-heptadecafluorodecyl)$_8$Si$_8$O$_{12}$ POSS (Fluorodecyl POSS or Fluorodecyl$_8$T$_8$). This method has been employed successfully to produce octahedral FluoroPOSS compounds possessing 3, 6, 8, 10, and 12 carbon atoms in each fluoroalkyl chain. Attempts to produce octahedral (3,3,3-trifluoropropyl)$_8$Si$_8$O$_{12}$ (Fluoropropyl POSS) *via* a similar condensation reaction of (3,3,3-trifluoropropyl)trichlorosilane resulted in a mixture of completely-condensed POSS cages possessing 8, 10, and 12 silicon atoms, respectively, which led to the use of the "corner-capping" method.

FluoroPOSS compounds are generally soluble in fluorinated solvents. Unlike most non-fluorinated POSS compounds, TGA analysis indicates that FluoroPOSS tend to volatilize, where no residue remains after heating under nitrogen or dry air, rather than decompose. Fluorodecyl POSS is the most stable compound, evaporating at well ~325 °C. FluoroPOSS compounds are also very dense, high molecular weight materials. For example, the molecular weight and density of Fluorodecyl POSS are 3993.54 g/mol and 2.067 g/cc, respectively. Several groups have developed and examined theoretical models for the structure [26], miscibility [27], and wetting behavior [28,6,29] of these compounds and their surfaces.

Because of their interesting properties, FluoroPOSS compounds have been examined for use in a variety of applications, including non-wetting and antibacterial fabrics and meshes [30-33] and ice-phobic surfaces [34]. However, the majority of research involving FluoroPOSS has centered around the idea of non-wetting polymers and surfaces [35-39,23,40,41,6,29,42]. Many groups have reported other compounds described as FluoroPOSS, Fluorinated POSS, F-POSS, or POSS-F, but these compounds are either hydrocarbon-surrounded POSS cages with a low number of fluoroalkyl groups [43-46], or non-fluorinated POSS compounds combined with fluorinated polymers [47-51], or both.

X.1.3 Design parameters

The design of super-repellent surfaces typically involves the manipulation of two key surface parameters, the substrate surface energy (γ_{sv}) and the surface roughness or texture [52-57]. A droplet of liquid on a textured substrate can adopt one of the following two configurations to minimize its overall free energy [58,2,55,56,59]. In the first case, as shown in Figs. 4A and 4B, the contacting liquid droplet may completely cover all of the substrate surface asperities, forming the so-called 'fully-wetted' interface. In this state, the apparent contact angles are calculated using the Wenzel relation [52], given as:

$$\cos\theta^* = r\cos\theta \tag{2}$$

Here r is the surface roughness defined as actual surface area / projected surface area. On the other hand, for an extremely rough surface, a 'composite' interface may lead to a lower overall free energy. In this case, the rough surface is not fully wetted by a liquid, and pockets of air remain trapped underneath the liquid droplet (see Figs. 4C and 4D). In contrast to a fully wetted interface, the composite interface typically leads to low contact angle hysteresis and low roll-off angles [3,60,54]. The apparent contact angle in this state is typically calculated using the Cassie-Baxter model [53], given as:

$$\cos\theta^* = r_\phi \phi_s \cos\theta - 1 + \phi_s \tag{3}$$

Here ϕ_s is the fraction of the projected area wet by the liquid, and r_ϕ is the roughness of the wetted area. When $\phi_s = 1$ (fully wetted surface), $r_\phi = r$, and the Cassie-Baxter relation reduces to the Wenzel relation. Extremely non-wetting surfaces must be able to support a composite interface with various contacting liquids, as the Cassie-Baxter state typically yields both high apparent contact angles and low contact angle hysteresis. In recent work, we [32,29,6] and others [61-64] have explained how *re-entrant surface texture*, in conjunction with surface chemistry and roughness, can be used to support a composite interface, even with extremely low surface tensions liquids such as various oils and alcohols.

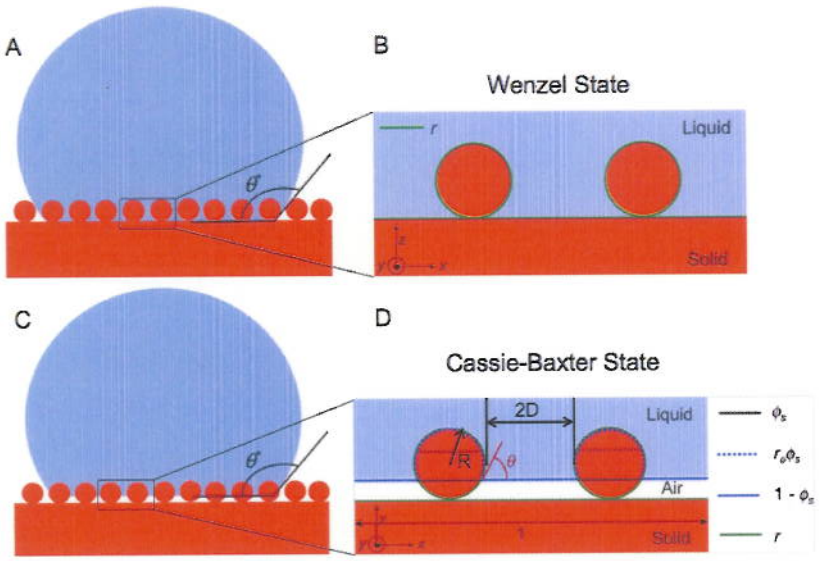

Fig. X.4 A. A schematic illustration of the Wenzel state with the liquid droplet filling in the various asperities present on the surface. **B.** A magnified view of the schematic shown in Fig. 2A. **C.** A schematic illustration of the Cassie-Baxter state with the liquid droplets sitting partially on the solid substrate and partially on pockets of air, forming a composite interface. **D.** A magnified view of the schematic shown in Fig. 2C. Note that the local contact angle for the liquid on the solid substrate is equal to the Young's contact angle θ.

The systematic design of non-wetting surfaces with any contacting liquid requires the parameterization of two important physical characteristics for a composite interface: The magnitude of the observed apparent contact angle θ^*, and the magnitude of the breakthrough pressure, i.e., the external pressure which when applied upon a contacting liquid can force a transition from the composite Cassie-Baxter state to the fully-wetted Wenzel state.

As mentioned earlier, the apparent contact angles for a composite interface are typically predicted using the Cassie-Baxter relation (Eq. 2). In our recent work [6,29] we discussed a design parameter, the spacing ratio D^*, which provides a dimensionless measure of the surface porosity. For substrates possessing a predominantly spherical or cylindrical texture, $D^* = (R+D)/R$, where R is the radius of the cylinders (or spheres) and $2D$ is the inter-cylinder spacing (see Fig. 4D). Based on this definition of the spacing ratio, the Cassie-Baxter relation (Eq. 2) may be re-written as:

$$\cos\theta^* = -1 + \frac{1}{D^*}\left[\sin\theta + (\pi - \theta)\cos\theta\right] \qquad (4)$$

Higher values of D^* correspond to a higher fraction of air in the composite interface. It is evident from Eq. 3 that θ^* increases with increasing values of D^*. In our recent work [32,29], we also discussed the robustness factor A^*, which is the ratio of the breakthrough pressure ($P_{breakthrough}$) to a reference pressure $P_{ref} = 2\gamma_{lv}/l_{cap}$. Here $l_{cap} = \sqrt{\gamma_{lv}/\rho g}$ is the capillary length for the liquid, ρ is the fluid density and g is the acceleration due to gravity. P_{ref} is close to the minimum possible pressure differential across a millimeter sized liquid droplet or puddle. As a consequence, any substrate on which the robustness factor $A^* \leq 1$ for a given contacting liquid, cannot support a composite interface. On the other hand, values of A^* significantly greater than unity imply the formation of a robust composite interface able to support high breakthrough pressures. For surfaces possessing a cylindrical texture, the robustness factor is given by the relation:

$$A^* = \frac{P_{breakthrough}}{P_{ref}} = \frac{Rl_{cap}}{D^2} \frac{(1-\cos\theta)}{(1+2(R/D)\sin\theta)} \tag{5}$$

The optimal superhydrophobic or superoleophobic surfaces are expected to simultaneously possess high contact angles and high breakthrough pressures, i.e. both $D^* >> 1$ and $A^* >> 1$.

X.2. Experimental

X.2.1 Materials

Asahiklin AK-225G (1,3-dichloro-1,1,2,2,3-pentafluoropropane) was purchased from Asahi Glass Co. PMMA (Mw = 540 kDa, PDI ≈ 2.2) was purchased from Scientific Polymer Products, Inc. Tecnoflon (BR9151), a commercial fluoro-elastomer, was obtained from Solvay-Solexis.

All other reagents were purchased from commercial sources and purified according to established procedures. [65]

X.2.2 FluoroPOSS synthesis

Fluorodecyl POSS synthesis [24,40,6]. 1H,1H,2H,2H-Heptadecafluorodecyltri-ethoxysilane (6.10 g), deionized water (0.27 g), and potassium hydroxide (2.088 mg) were added to a 10 ml volumetric flask. The balance of the volume to 10 ml was filled with ethanol. The contents were transferred to a 25 ml round bottom flask with a Teflon covered magnetic stir bar. The contents were stirred at room temperature overnight under nitrogen. A fine white powder was formed. The

product was rinsed with ethanol and dried. A 94.3% yield of pure 1H,1H,2H,2H-heptadecafluorodecyl$_8$T$_8$ was obtained. ^{29}Si NMR ($(CD_3)_2CO$, 59.6 MHz): δ = -67.0 ppm.

X.2.3 FluoroPOSS composite preparation

X.2.3.1 Spin-cast surfaces

Both the polymer and fluoroPOSS were dissolved in a common solvent, Asahiklin AK-225, at a concentration of 5 mg/ml, and the rotation speed during spincoating was set at 900 rpm.

X.2.3.2 Electrospun surfaces

Both the polymer and fluoroPOSS were dissolved in Asahiklin AK-225 at a concentration of ~ 5 wt%. The solution was then electrospun using a custom-built apparatus with the flow rate, plate-to-plate distance and voltage set to 0.05 ml/min, 25 cm and 20 kV, respectively.

X.2.3.3 Dip-coated surfaces

For the dip-coating process, a solution of fluorodecyl POSS (50 wt%) and Tecnoflon in Asahiklin AK-225G was prepared at an overall solid concentration of 10 mg/mL. The use of Tecnoflon as a polymeric binder inhibits the crystallization of fluorodecyl POSS, and yields a more conformal and elastomeric coating. The substrate was then immersed in the fluorodecyl POSS-Tecnoflon solution. After 5 min, the substrate was removed from the solution and placed to dry in a vacuum oven for 30 min at a temperature of 60 °C.

X.2.4 Contact angle analysis

The contact angles for various liquids were measured using a contact angle goniometer, VCA2000 (AST Inc.). The advancing contact angle was measured by advancing a small volume of the probing liquid (typically 2-4 µl) on to the surface, using a syringe. The receding contact angle was measured by slowly removing the probing liquid from a drop already on the surface. For each sample a minimum of four different readings were recorded. Typical error in measurements was ~2°.

X.2.5 Microscopy

X.2.5.1 Atomic Force Microscopy (AFM)

Atomic force microscopy (AFM) was conducted on a Nanoscope IV controller (3100 SPM Head) in tapping mode. Etched Silicon probes of nominal spring resonance 300 kHz (spring constant approx. 0.3 mN/m) were used for light

tapping (driving amplitude ca 1.1 V) of varying section size at 1–2 Hz collection times (512 points/line).

X.2.5.2 Scanning Electron Microscopy (SEM)

A JEOL-6060SEM (JEOL Ltd., Japan) scanning electron microscope (SEM) was used for imaging. Before imaging, the electrospun surfaces were sputter-coated with a 5-10 nm layer of gold by use of a Desk II cold sputter/etch unit (Denton Vacuum LLC).

X.3. Results and Discussion

X.3.1 FluoroPOSS properties

Zisman showed that the surface energy for organic molecules decreases with an increase in the degree of fluorination, and as a result the surface energy for $-CH_3$ > $-CH_2F$ > $-CHF_2$ > $-CF_3$ moieties. The high concentration of perfluorinated carbon atoms in the alkyl chains surrounding each FluoroPOSS cage leads to extremely low surface energy values for these molecules.[66,67,24] As synthesized, fluorodecyl POSS molecules possess one of the lowest known solid surface energies ($\gamma_{sv} \approx 8$ mN/m). [4-6] In comparison, Teflon, has a surface energy of $\gamma_{sv} \approx 17$ mN/m. A film of fluorodecyl POSS, spincoated on a Si wafer and having an rms roughness of 3.5 nm (this corresponds to a Wenzel surface roughness $r = 1.005$) has an advancing (θ_{adv}) and receding (θ_{rec}) contact angle of $124.5 \pm 1.2°$. This is one of the highest water contact angles reported for a smooth substrate [5], and emphasizes the extremely low surface energy of the fluorodecyl POSS molecules.

X.3.2 FluoroPOSS composites

The addition of fluorodecyl POSS molecules to different polymers leads to a rapid decrease in the overall surface energy of the synthesized composites, and also provides a facile route to systematically tune the surface energy of the produced composite over a very wide range. For example, we studied composites formed by blending fluorodecyl POSS molecules with a relatively hydrophilic polymer, poly(methylmethacrylate) (PMMA). The addition of fluorodecyl POSS molecules allowed us to systematically tune the surface energy of the produced composites from $\gamma_{sv} = 9 - 35$ mN/m.[67,68] Fig. 5A shows AFM phase images for various spin-coated blends of PMMA and fluorodecyl POSS. A comparison between the phase images for neat PMMA and for PMMA+1.9 wt% fluorodecyl POSS indicates significant surface segregation (or blooming) of fluorodecyl POSS molecules towards the air interface, due to their extremely low surface energy [6].

As a result, only a small amount of fluorodecyl POSS (~ 10 wt%) is needed to sufficiently cover the surface of the spin-coated blend. Fig. 5B shows the advancing and receding contact angles for the various spin-coated PMMA+ fluorodecyl POSS blends. For fluorodecyl POSS, concentrations greater than ~ 10 wt%, both the advancing and receding contact angles plateau to ~ $\theta_{adv} = \theta_{rec} =$ 123°.

Fig. 5C shows the corresponding contact angles on electrospun fabric surfaces possessing the so-called beads-on-a-string morphology. The inset shows the morphology for a typical electrospun mat, and highlights both the porosity and the re-entrant curvature present in the fabricated surfaces. It is clear that electrospun blend surfaces containing greater than ~ 10 wt% POSS are superhydrophobic, displaying both θ^*_{adv}, $\theta^*_{rec} > 150°$.

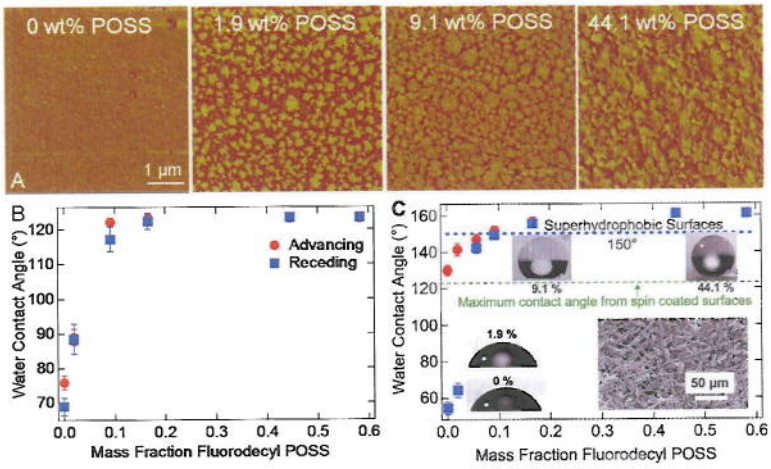

Fig. X.5 A. AFM phase images for neat PMMA and PMMA blends with fluorodecyl POSS. The phase angle scale on the AFM images is 0-10° for the 0%, 9.1%, 44 wt% POSS images and 0-90° for the 1.9 wt% POSS image. **B.** The advancing and receding contact angles for water on spin coated surfaces composed of neat PMMA and its blends with fluorodecyl POSS. **C.** The apparent advancing (red dots) and receding (blue dots) contact angles for water on various electrospun surfaces composed on PMMA and fluorodecyl POSS. The inset shows an SEM micrograph for an electrospun surface composed of PMMA + 9.1 wt % fluorodecyl POSS. Images adapted from previous work.[67]

The re-entrant curvature inherently present in the electrospun fabric surface creates the potential to form a composite interface with any liquid with a Young's contact angle greater than 0°, provided the robustness factor $A^* > 1$ [32,29]. Fig. 6A shows the apparent advancing and receding contact angles on the electrospun surfaces containing 16.7 wt% and 44.1 wt% fluorodecyl POSS, for a series of

liquids with surface tension values in the range of γ_{lv} = 20.1 – 72.1 mN/m. Due to the high porosity inherent in the electrospun mat (D^* = 9), the synthesized electrospun surfaces display extremely high apparent contact angles with a wide range of liquids (see Fig. 6B). For example, for hexadecane (γ_{lv} = 27.5 mN/m), θ^*_{adv} = 153° and θ^*_{rec} = 141°. Further, due to their extremely small dimensions (R ~ 500 nm), the electrospun fibers also possess very high values of robustness factor [29]. For example, for the electrospun fibers containing 44.4 wt% fluorodecyl POSS, A^* = 40 with hexadecane.

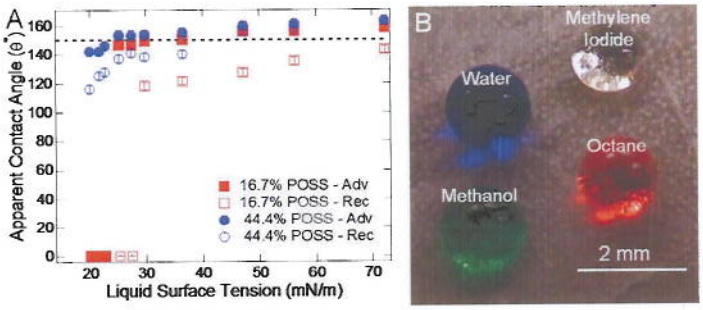

Fig. X.6 A. The apparent advancing (filled symbols) and receding (open symbols) contact angles as a function of the liquid surface tension for the electrospun surfaces possessing a beads-on-a-string morphology. The electrospun surfaces are composed of PMMA with either 16.7 wt% or 44.1 wt% fluorodecyl POSS. **B.** Droplets of water (γ_{lv} = 72.1mN/m), methylene iodide (γ_{lv} = 50.1 mN/m), methanol (γ_{lv} = 22.7 mN/m) and octane (γ_{lv} = 21.7 mN/m) on an electrospun surface composed of PMMA + 44 wt% fluorodecyl POSS, possessing a beads-on-a-string morphology. The electrospun substrate is able to support a composite interface with all contacting liquids, as indicated by the presence of a reflective surface visible underneath all droplets.[6] Images adapted from previous work.[29]

As mentioned previously, there are no naturally occurring oleophobic or superoleophobic surfaces. The inset in Fig. 7A shows droplets of rapeseed oil (γ_{lv} = 35.7 mN/m) on top of a lotus leaf. Evaluating the magnitude of the robustness factor ($A^* << 1$) helps explain why rapeseed oil spontaneously wets the leaf structure in spite of the presence of re-entrant texture [29]. To allow the leaf surface to support a composite interface with low surface tension liquids such as various oils, it is necessary to significantly increase the value of the robustness factor A^*. Based on Equation 5, for a fixed substrate texture, it is clear that the magnitude of A^* is most easily induced by increasing the value for the Young's contact angle θ. We use the dip-coating process to provide a conformal coating of fluorodecyl POSS molecules on top of the lotus leaf surface. This leads to a significant increase in the magnitude of the Young's contact angle (θ = 86°) and correspondingly the value of the robustness factor on the dip-coated lotus leaf (A^* = 26) [29]. As a result, the dip-coated lotus leaf is readily able to support a

composite interface with rapeseed oil and display high apparent contact angles, as illustrated in the inset of Fig. 7B. Fig. 7A and 7B compare the surface texture of the lotus leaf before and after the dip-coating process. It is clear that the dip-coating process preserves the inherent surface texture of the lotus leaf.

Recognizing the presence of re-entrant surface features in commercial fabrics, the dip-coating process was used to deliver a coating of fluorodecyl POSS molecules onto the fabric surface, bestowing superoleophobicity. Note that Tecnoflon, a fluoroelastomer binder, was added to the dip-coating solution to inhibit the formation of fluorodecyl POSS crystallites and yield a more conformal and elastomeric coating.

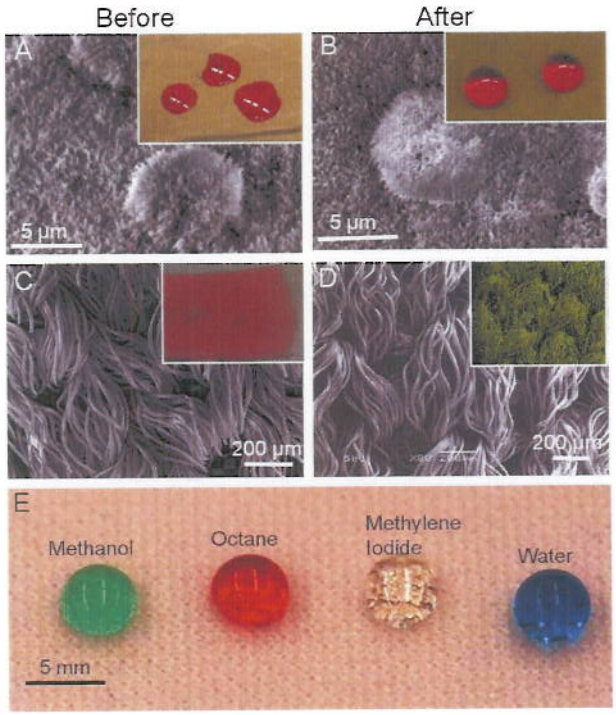

Fig. X.7 A. An SEM image of the lotus leaf surface before the dip-coating process. The inset shows the extremely low apparent contact angle ($\theta^* \sim 10°$) observed for rapeseed oil (colored red) on top of the lotus leaf surface. **B.** An SEM image of the lotus leaf surface after the dip-coating process. The inset shows the high apparent contact angles observed for rapeseed oil on the dip-coated lotus leaf surface ($\theta^* = 145°$). **C.** An SEM image illustrating the morphology of a commercially available polyester fabric. The inset shows that a droplet of hexadecane ($\gamma_{lv} = 27.5$ mN/m) readily wets the fabric surface. **D.** An SEM image illustrating the morphology of the

polyester fabric after the dip-coating process. The inset shows the elemental mapping for fluorine on the dip-coated fabric surface, obtained using EDAXS. **E.** Droplets of water (γ_{lv} = 72.1mN/m), methylene iodide (γ_{lv} = 50.1 mN/m), methanol (γ_{lv} = 22.7 mN/m) and octane (γ_{lv} = 21.7 mN/m) on the dip-coated fabric surface. Images reproduced from previous work.[32]

Fig. 7C shows an SEM micrograph for a commercially available polyester fabric, and highlights both the porosity (D^* = 6) and the re-entrant curvature of the fabric surface. The inset in Fig. 7C shows that a drop of rapeseed oil readily wets the as-obtained fabric surface. Fig. 7D illustrates the details of the polyester fabric surface after the dip-coating process. The inset in Fig. 7D shows the elemental mapping for fluorine on the dip-coated fabric surface, obtained using EDAXS (Energy Dispersive X-Ray Scattering). It is clear from this image that the dip-coating process allows for the complete and conformal coating of the fabric surface by the fluorodecyl POSS molecules. After the dip-coating process, as shown in Fig. 7E, the fabric surface is able to support a composite interface, and display extremely high apparent contact angles with a wide range of liquids including octane (γ_{lv} = 21.7 mN/m; A^* = 2.5).

X.4. Conclusions

In the design of non-wetting surfaces, surface texture has been found to be of equal or greater importance than surface free energy and surface roughness characteristics, which are considered critical for the creation of such surfaces. This is especially the case if the surface is desired to repel low surface tension liquids, such as different oils or alcohols. The low surface energy characteristics of fluorinated Polyhedral Oligomeric SilSesquioxanes (FluoroPOSS), as well as their octahedral structure, make them desirable compounds for use in the production of non-wetting surfaces. Wetting-resistant surfaces containing FluoroPOSS were produced by a variety of methods. Design parameters were also developed to aid the rational design of non-wetting surfaces. The spacing ratio, D^*, provides a dimensionless measure of surface porosity, while the robustness factor, A^*, is a measure of a surface's resistance to liquid breakthrough. The most favorable non-wetting surface would, therefore, possess high values of both D^* and A^* simultaneously, indicating high contact angles as well as high breakthrough pressures. Production of wetting-resistant surfaces may involve techniques that specifically incorporate all three factors critical for wetting-resistance, such as electrospinning. Alternatively, substrates containing the desired surface texture may be modified to bestow wetting-resistance, as seen in the dip-coating of commercial fabrics.

Acknowledgments

We thank Dr. Charles Y-C. Lee and the Air Force Office of Scientific Research (AFOSR) for financial support under grants FA9550-10-1-0523 and LRIR-92PL0COR. We also thank the Air Force Research Laboratory, Propulsion Directorate for their financial support. We also thank Prof. Robert E. Cohen, Prof. Gareth H. McKinley, and Prof. Wonjae Choi for their contributions to this work and helpful conversations.

References

1. Young T (1805) An Essay on the Cohesion of Fluids. Philos Trans R Soc London 95:65

2. Shuttleworth R, Bailey GLJ (1948) The spreading of a liquid over a rough solid. Discuss Faraday Soc 3:16-22. doi:10.1039/DF9480300016

3. Chen W, Fadeev AY, Hsieh MC, Oner D, Youngblood J, McCarthy TJ (1999) Ultrahydrophobic and Ultralyophobic Surfaces: Some Comments and Examples. Langmuir 15 (10):3395-3399

4. Genzer J, Efimenko K (2000) Creating Long-Lived Superhydrophobic Polymer Surfaces Through Mechanically Assembled Monolayers. Science 290 (5499):2130-2133. doi:10.1126/science.290.5499.2130

5. Nishino T, Meguro M, Nakamae K, Matsushita M, Ueda Y (1999) The lowest surface free energy based on -CF3 alignment. Langmuir 15 (13):4321-4323

6. Tuteja A, Choi W, Ma ML, Mabry JM, Mazzella SA, Rutledge GC, McKinley GH, Cohen RE (2007) Designing superoleophobic surfaces. Science 318:1618-1622. doi:10.1126/science.1148326

7. Barthlott W, Neinhuis C (1997) Purity of the sacred lotus, or escape from contamination in biological surfaces. Planta 202 (1):1-8

8. Herminghaus S (2000) Roughness-induced non-wetting. Europhys Lett 52 (2):165-170

9. Neinhuis C, Barthlott W (1997) Characterization and distribution of water-repellent, self-cleaning plant surfaces. Ann Botany 79 (6):667-677

10. Hu DL, Chan B, Bush JWM (2003) The hydrodynamics of water strider locomotion. Nature 424 (6949):663

11. Hu DL, Bush JWM (2005) Meniscus-climbing insects. Nature 437 (7059):733

12. Gao X, Jiang L (2004) Biophysics: Water-repellent legs of water striders. Nature 432 (7013):36

13. Autumn K, Liang YA, Hsieh ST, Zesch W, Chan WP, Kenny TW, Fearing R, Full RJ (2000) Adhesive force of a single gecko foot-hair. Nature 405 (6787):681-685

14. Genzer J, Efimenko K (2006) Recent developments in superhydrophobic surfaces and their relevance to marine fouling: a review. Biofouling 22 (5):339-360

15. Parker AR, Lawrence CR (2001) Water capture by a desert beetle. Nature 414 (6859):33

16. Wagner T, Neinhuis C, Barthlott W (1996) Wettability and contaminability of insect wings as a function of their surface sculptures. Acta Zool 77 (3):213-225

17. Choi W, Tuteja A, Mabry JM, Cohen RE, McKinley GH (2009) A modified Cassie-Baxter relationship to explain contact angle hysteresis and anisotropy on non-wetting textured surfaces. Journal of Colloid and Interface Science 339 (1):208-216

18. POSS is a registered trademark of Hybrid Plastics Inc., Hattiesburg, MS 39401

19. Pielichowski K, Njuguna J, Janowski B, Pielichowski J (2006) Polyhedral Oligomeric Silsesquioxanes (POSS)-Containing Nanohybrid Polymers. In: Supramolecular Polymers Polymeric Betains Oligomers, vol 201. Advances in Polymer Science. Springer Berlin / Heidelberg, pp 225-296. doi:10.1007/12_077

20. Lickiss PD, Rataboul F (2008) Chapter 1 Fully Condensed Polyhedral Oligosilsesquioxanes (POSS): From Synthesis to Application. In: Anthony FH, Mark JF (eds) Advances in Organometallic Chemistry, vol Volume 57. Academic Press, pp 1-116

21. Cordes DB, Lickiss PD, Rataboul F (2010) Recent Developments in the Chemistry of Cubic Polyhedral Oligosilsesquioxanes. Chemical Reviews 110 (4):2081-2173. doi:10.1021/cr900201r

22. Iacono ST, Vij A, Grabow W, Smith JDW, Mabry JM (2007) Facile synthesis of hydrophobic fluoroalkyl functionalized silsesquioxane nanostructures. Chemical Communications (47):4992-4994

23. Koh K, Sugiyama S, Morinaga T, Ohno K, Tsujii Y, Fukuda T, Yamahiro M, Iijima T, Oikawa H, Watanabe K, Miyashita T (2005) Precision Synthesis of a Fluorinated Polyhedral Oligomeric Silsesquioxane-Terminated Polymer and Surface Characterization of Its Blend Film with Poly(methyl methacrylate). Macromolecules 38 (4):1264-1270. doi:10.1021/ma047636l

24. Mabry JM, Vij A, Iacono ST, Viers BD (2008) Fluorinated Polyhedral Oligomeric Silsesquioxanes (F-POSS). Ange Chem Int Ed 47 (22):4137-4140

25. Xu J, Li X, Cho CM, Toh CL, Shen L, Mya KY, Lu X, He C (2009) Polyhedral oligomeric silsesquioxanes tethered with perfluoroalkylthioether corner groups: Facile synthesis and enhancement of hydrophobicity of their polymer blends. Journal of Materials Chemistry 19 (27):4740-4745

26. Anderson SE, Bodzin DJ, Haddad TS, Boatz JA, Mabry JM, Mitchell C, Bowers MT (2008) Structural Investigation of Encapsulated Fluoride in

Polyhedral Oligomeric Silsesquioxane Cages Using Ion Mobility Mass Spectrometry and Molecular Mechanics. Chemistry of Materials 20 (13):4299-4309. doi:10.1021/cm800058z

27. Zeng F-l, et al. (2009) Molecular simulations of the miscibility in binary mixtures of PVDF and POSS compounds. Modelling and Simulation in Materials Science and Engineering 17 (7):075002

28. Losada M, Mackie K, Osborne JH, Chaudhuri S (2010) Understanding Nanoscale Wetting using Dynamic Local Contact Angle Method. In: Trasatti SPIJ (ed) Light Weight Metal Corrosion and Modeling for Corrosion Prevention, Life Prediction and Assessment, vol 138. Advanced Materials Research. pp 107-116. doi:10.4028/http://www.scientific.net/AMR.138.107

29. Tuteja A, Choi W, Mabry JM, McKinley GH, Cohen RE (2008) Robust omniphobic surfaces. Proceedings of the National Academy of Sciences of the United States of America 105 (47):18200-18205. doi:10.1073/pnas.0804872105

30. Chhatre SS, Choi W, Tuteja A, Park K-C, Mabry JM, McKinley GH, Cohen RE (2009) Scale Dependence of Omniphobic Mesh Surfaces. Langmuir 26 (6):4027-4035. doi:10.1021/la903489r

31. Chhatre SS, Tuteja A, Choi W, Revaux A, Smith D, Mabry JM, McKinley GH, Cohen RE (2009) Thermal Annealing Treatment to Achieve Switchable and Reversible Oleophobicity on Fabrics. Langmuir 25 (23):13625-13632. doi:10.1021/la901997s

32. Choi W, Tuteja A, Chhatre S, Mabry JM, Cohen RE, McKinley GH (2009) Fabrics with Tunable Oleophobicity. Advanced Materials 21 (21):2190-2195. doi:10.1002/adma.200802502

33. Vilcnik A, Jerman I, Såurca Vuk A, Kozåelj M, Orel B, Tomsåicå B, Simoncåicå B, Kovacå J (2009) Structural Properties and Antibacterial Effects of Hydrophobic and Oleophobic Sol-Gel Coatings for Cotton Fabrics. Langmuir 25 (10):5869-5880. doi:10.1021/la803742c

34. Meuler AJ, Smith JD, Varanasi KK, Mabry JM, McKinley GH, Cohen RE (2010) Relationships between Water Wettability and Ice Adhesion. ACS Applied Materials & Interfaces 2 (11):3100-3110. doi:10.1021/am1006035

35. Chhatre SS, Guardado JO, Moore BM, Haddad TS, Mabry JM, McKinley GH, Cohen RE (2010) Fluoroalkylated Silicon-Containing Surfaces,àíEstimation of Solid-Surface Energy. ACS Applied Materials & Interfaces 2 (12):3544-3554. doi:10.1021/am100729j

36. Iacono Scott T, Budy Stephen M, Mabry Joseph M, Smith Dennis W (2010) Polyhedral Oligomeric Silsesquioxane-Functionalized Perfluorocyclobutyl Aryl Ether Polymers. In: Advances in Silicones and Silicone-Modified Materials, vol 1051. ACS Symposium Series, vol 1051. American Chemical Society, pp 195-209. doi:doi:10.1021/bk-2010-1051.ch016
10.1021/bk-2010-1051.ch016

37. Iacono ST, Budy SM, Mabry JM, Smith Jr DW (2007) Synthesis, characterization, and properties of chain terminated polyhedral oligomeric silsesquioxane-functionalized perfluorocyclobutyl aryl ether copolymers. Polymer 48 (16):4637-4645. doi:10.1016/j.polymer.2007.06.022

38. Iacono ST, Budy SM, Smith DW, Mabry JM (2010) Preparation of composite fluoropolymers with enhanced dewetting using fluorinated silsesquioxanes as drop-in modifiers. Journal of Materials Chemistry 20 (15):2979-2984

39. Iacono ST, Peloquin AJ, Dennis W. Smith J, Mabry JM (2011) Fluorinated Polyhedral Oligosilsesquioxane Surfaces and Superhydrophobicity. In: Hartmann-Thompson C (ed) Applications of Polyhedral Oligomeric Silsesquioxanes. 1st Edition edn. Springer, p 392

40. Mabry Joseph M, Vij A, Viers Brent D, Grabow Wade W, Marchant D, Iacono Scott T, Ruth Patrick N, Vij I (2007) Hydrophobic Silsesquioxane Nanoparticles and Nanocomposite Surfaces. In: Science and Technology of Silicones and Silicone-Modified Materials, vol 964. ACS Symposium Series, vol 964. American Chemical Society, pp 290-300. doi:doi:10.1021/bk-2007-0964.ch018
10.1021/bk-2007-0964.ch018

41. Srinivasan S, Chhatre SS, Mabry JM, Cohen RE, McKinley GH (2011) Solution spraying of poly(methyl methacrylate) blends to fabricate microtextured, superoleophobic surfaces. Polymer 52 (14):3209-3218. doi:10.1016/j.polymer.2011.05.008

42. Xue Y, Wang H, Zhao Y, Dai L, Feng L, Wang X, Lin T (2010) Magnetic Liquid Marbles: A "Precise" Miniature Reactor. Advanced Materials 22 (43):4814-4818. doi:10.1002/adma.201001898

43. Dai L, Yang C, Xu Y, Deng Y, Chen J, Galy J, Gérard J-F (2010) Preparation of novel methyl methacrylate/fluorinated silsesquioxane copolymer film with low surface energy. SCIENCE CHINA Chemistry 53 (9):2000-2005. doi:10.1007/s11426-010-4070-4

44. Dodiuk H, Rios PF, Dotan A, Kenig S (2007) Hydrophobic and self-cleaning coatings. Polymers for Advanced Technologies 18 (9):746-750. doi:10.1002/pat.957

45. Kannan AG, Choudhury NR, Dutta N (2009) Fluoro-silsesquioxane-urethane Hybrid for Thin Film Applications. ACS Applied Materials & Interfaces 1 (2):336-347. doi:10.1021/am800056p

46. Rios PF, Dodiuk H, Kenig S, McCarthy S, Dotan A (2007) Transparent ultra-hydrophobic surfaces. Journal of Adhesion Science and Technology 21 (5-6):399-408. doi:10.1163/156856107780474975

47. Gao Y, He C, Huang Y, Qing F-L (2010) Novel water and oil repellent POSS-based organic/inorganic nanomaterial: Preparation, characterization and application to cotton fabrics. Polymer 51 (25):5997-6004. doi:10.1016/j.polymer.2010.10.020

48. Iacono ST, Budy SM, Mabry JM, Smith DW (2007) Synthesis, Characterization, and Surface Morphology of Pendant Polyhedral Oligomeric Silsesquioxane Perfluorocyclobutyl Aryl Ether Copolymers. Macromolecules 40 (26):9517-9522. doi:10.1021/ma071732f

49. Sawada H, Yoshioka H, Ohashi R, Kawase T (2002) Synthesis and properties of novel fluoroalkyl end-capped oligomers containing silsesquioxane segments. Journal of Applied Polymer Science 86 (14):3486-3493. doi:10.1002/app.10859

50. Song L, Peng S, Shu Y (2011) Preparation of A Novel Functionated POSS Nano-particle Bearing the Perfluoro Aryl Ether Dendron. In: Liu XHJZYHJT (ed) Manufacturing Processes and Systems, Pts 1-2, vol 148-149. Advanced Materials Research. pp 1212-1216. doi:10.4028/http://www.scientific.net/AMR.148-149.1212

51. Vasilopoulou M, et al. (2005) Characterization of various low- k dielectrics for possible use in applications at temperatures below 160 ¬∞C. Journal of Physics: Conference Series 10 (1):218

52. Wenzel RN (1936) Resistance of solid surfaces to wetting by water. Ind & Eng Chem 28:988–994

53. Cassie ABD, Baxter S (1944) Wettability of porous surfaces. Trans Faraday Soc 40: 546–551

54. Callies M, Quéré D (2005) On water repellency. Soft Mat 1 (1):55-61

55. Marmur A (2003) Wetting on Hydrophobic Rough Surfaces: To Be Heterogeneous or Not To Be? Langmuir 19 (20):8343-8348

56. Nosonovsky M (2007) Multiscale Roughness and Stability of Superhydrophobic Biomimetic Interfaces. Langmuir 23 (6):3157-3161

57. Quéré D (2002) Rough ideas on wetting. Physica A-Stat Mech & Appl 313 (1-2):32-46

58. Johnson RE, Dettre RH (1964) Contact angle hysteresis. In Contact Angle, Wettability and Adhesion, ACS Advances in Chemistry Series., vol 43. American Chemical Society, Washington, DC.

59. Patankar NA (2003) On the Modeling of Hydrophobic Contact Angles on Rough Surfaces. Langmuir 19 (4):1249-1253

60. Lafuma A, Quéré D (2003) Superhydrophobic states. Nature Mater 2 (7):457-460

61. Ahuja A, Taylor JA, Lifton V, Sidorenko AA, Salamon TR, Lobaton EJ, Kolodner P, Krupenkin TN (2008) Nanonails: A simple geometrical approach to electrically tunable superlyophobic surfaces. Langmuir 24 (1):9-14. doi:10.1021/la702327z

62. Cao L, Price TP, Weiss M, Gao D (2008) Super Water- and Oil-Repellent Surfaces on Intrinsically Hydrophilic and Oleophilic Porous Silicon Films. Langmuir 24 (5):1640-1643. doi:10.1021/la703401f

63. Leng B, Shao Z, de With G, Ming W (2009) Superoleophobic Cotton Textiles. Langmuir 25 (4):2456-2460. doi:10.1021/la8031144

64. Marmur A (2008) From Hygrophilic to Superhygrophobic: Theoretical Conditions for Making High-Contact-Angle Surfaces from Low-Contact-Angle Materials. Langmuir 24 (14):7573-7579. doi:10.1021/la800304r

65. Armarego WLF, Chai CLL (2009) Purification of Laboratory Chemicals (Sixth Edition). Butterworth-Heinemann, Oxford. doi:10.1016/b978-1-85617-567-8.50004-4

66. Zisman WA (1964) Relation of the equilibrium contact angle to liquid and solid construction. In Contact Angle, Wettability and Adhesion, ACS Advances in Chemistry Series., vol 43. American Chemical Society, Washington, DC.

67. Tuteja A, Choi W, Ma ML, Mabry JM, Mazzella SA, Rutledge GC, McKinley GH, Cohen RE (2007) Designing superoleophobic surfaces. Science 318 (5856):1618-1622

68. Tuteja A, Choi W, Mabry JM, McKinley GH, Cohen RE (2008) Engineering robust omniphobic surfaces. PNAS 105 (47):18200-18205